LAr20 Reference Design 1b

Liquid argon TPC in a Vacuum Insulated Cryostat

UCLA Team

Introduction

The 1b LAr method follows the ICARUS detector in a broad concept, but is a modular with high fiducial to total argon ratio. The LANNDD concept Fig. 1 shows one of the drawings that has been presented for DUSEL and to the recent UCLA DOE review—the LANNDD detection concept (Fig. 1)

The ICARUS collaboration has operated a 300 ton system in Pavia in 2001 and is ready to operate the 600 ton detector at the Gran Sasso Laboratory now. The ICARUS group believes it is necessary to evacuate the detector system (with all the components in place) to remove the impurities in order to reach 10^{-1} ppb as was demonstrated in the Pavia run. The current 600 ton detector is under vacuum as of now in Gran Sasso. For the drift distances assumed in the DUSEL detector, a conservative purity would be 10^{-2} ppb. Until otherwise demonstrated on a similar scale (300 tons), we assume such a system should be evacuated.

We now turn to the design for the 20kT LAr detector at a shallow site. We assume the site can be reached by large trucks. This will greatly reduce the cost of the welding that would be needed for the vacuum insulation panels for the deep site and possibly the overall detector.

The cost estimate is based on the shallow site but the detector itself is virtually identical to the deeper site with associated installation cost higher. Which will be discussed in the reference 2B doc.

1. Detector Design Criteria

We consider the basic particle detection technique of the liquid argon TPC as well-established. Possible improvements can be produced essentially about readout electronics (cold front-end electronics to reduce the cable capacity load), when it will be recognized as ultra reliable solution. In competition/alternative with it, we propose an R&D dedicated to low capacitance, low heat conducting signal lines, 1.5-2 m long, with cold and warm multi-channel feedthroughs, to connect each wire to a warm preamplifier accessible from outside in any moment for reparation/substitution.

Our main concerns are about the efficiency, safety, and costs of an underground cryostat for the relevant liquid argon volume.

The present solution prefers to invest more resources on the cryostat, in any case unavoidable for safety, to get a quite, safe and economic operation during tenths of years. We expect a minimized global cost if we include the operation/maintenance costs. Vacuum insulation, combined with super-insulation layers, is 10-30 times more efficient than passive insulation. For a cryostat 20 m wide, 20 m high and 40 m long, we have a surface of 4'000 m^2 exposed to heat input. This means a total heat input of 3.7 kW (2.5 kW by radiation with vacuum + superinsulation and 1.2 kW by conduction in the thermal bridges) and a heat production in the underground cavern of ~40 kW if the cooling is provided by cryogenerators. With passive insulation the heat input can reach 24-70 kW with 400-1200 kW for the heat produced to compensate it (cooling of the cavern by water + fresh air becomes unavoidable).

Vacuum insulation is combined with the possibility to evacuate the inner vessel before filling by argon. This will result in a quicker and controlled achievement of the liquid argon purity at level of 10^{-10}-10^{-11} p/p of electronegative impurities allowing the configuration of the TPC with cathode-anode distances of the order of 2.5-5 meters and a minimized number of wire chambers.

Interferences between inner detector (wire chambers, cathodes and field shaping electrodes), cryostat, purification system, temperature stabilization circuitry and beam (direction and energy spectrum) as well as construction and assembling procedures have been matter for deciding the main features of this project.

2. Cryostat Structure

This design proposes a vacuum insulated, parallelepiped shaped cryostat for a 20-kton liquid argon TPC detector (Figure 1).

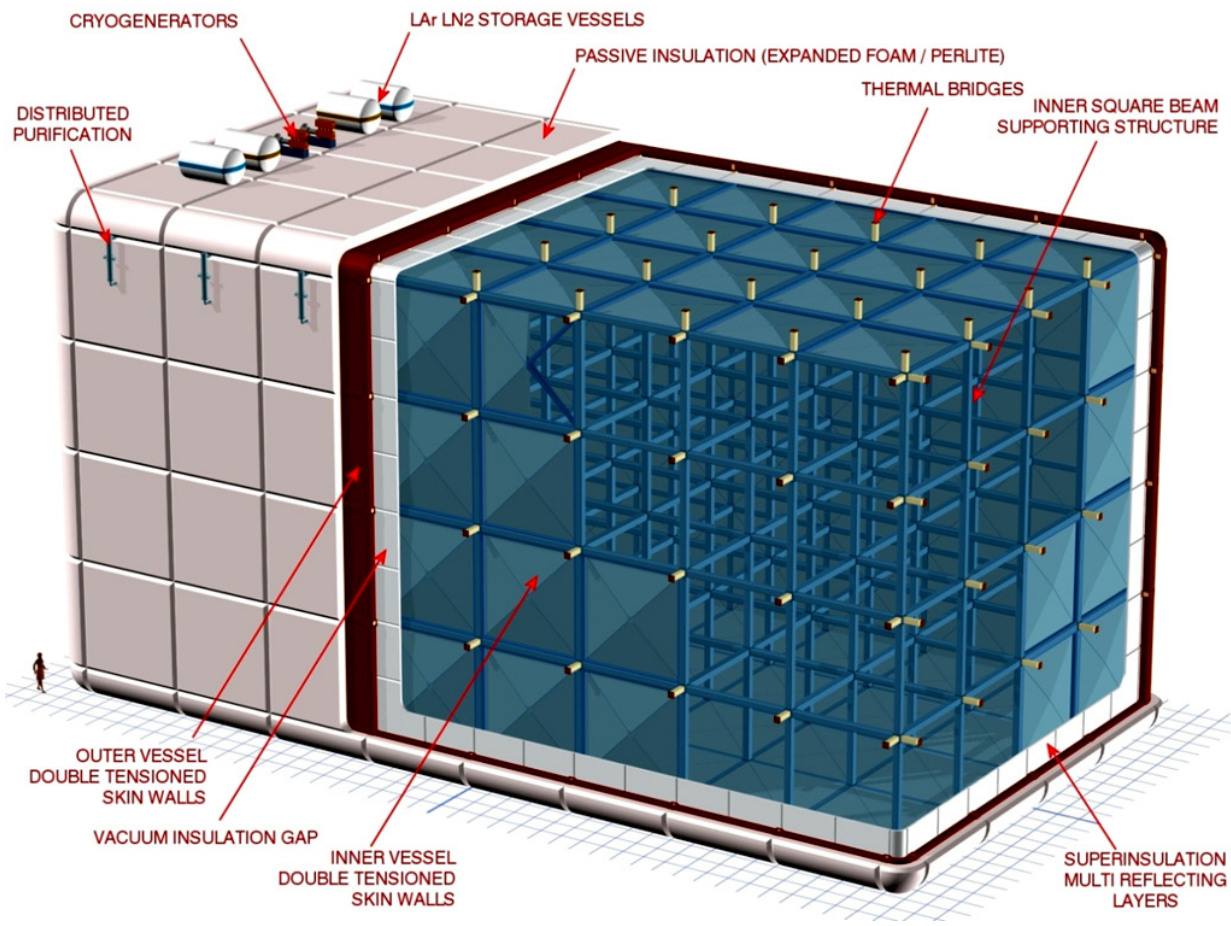

Figure 1

Vacuum insulation is obtained by an inner and an outer vessel, with vacuum in between. A 3-dimensional lattice structure (L×L×L), made by square stainless steel tubes, inside the inner vessel, provides the required stiffness to maintain flat the inner vessel walls. This kind of structure allows a flexible sizing of the full detector to adapt it to the realistic reachable sizes of the underground cavern, by arranging the configuration of the lattice structure and by defining the unit lattice cell dimension L (4 – 5 meter). Cryostat sizes for L = 5 m are reported in Figure 2 and 3.

Inner vessel is obtained by mounting double-skin square panels on the outer faces of the 3-d lattice structure. The outer vessel is obtained by replicating the inner vessel outer faces, offsetting them by a distance that allow man passage (for inspection and for wrapping the inner

vessel by superinsulation layers), and linking them on the corners by curved double skin panels. Outer vessel walls are kept flat by insulating beams (thermal bridges) inserted between the outer wall frames and the inner vessel lattice structure. Thermal bridges are equipped with compression springs and are connected to the outer vessel by sliding feet to cope with the thermal shrinkage of the inner vessel when filled by liquid argon.

The geometry of the double-skin panels is a matter of optimization by finite element analysis and by a full scale test with pressurized water. Different solutions have been studied, as pre-tensioned skins compressed in the middle or double sail skins and should be matter of a dedicated R&D program.

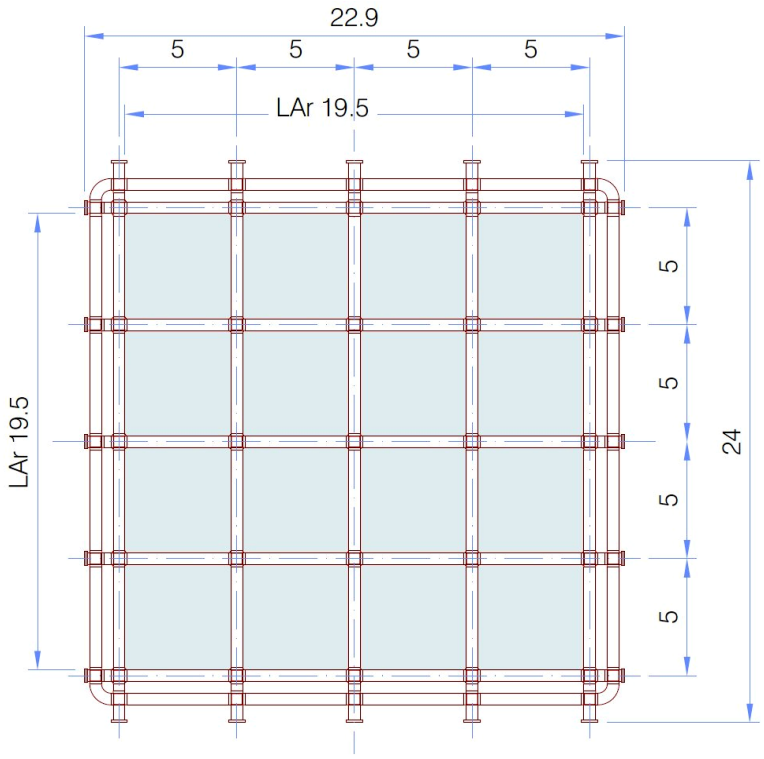

Figure 2

The inner vessel is wrapped by 30-60 layer superinsulation. This solution can limit the heat input to 0.6 watt/m².

The inner volume of the lattice structure beams and of the double skin walls is filled by liquid nitrogen to provide **initial cooling** and distributed **thermal stabilization** of the liquid argon. Eventual separated in level independent LN_2 circulations are foreseen to minimize thermal currents in liquid argon that could induce microphonic noise on the chamber wires.

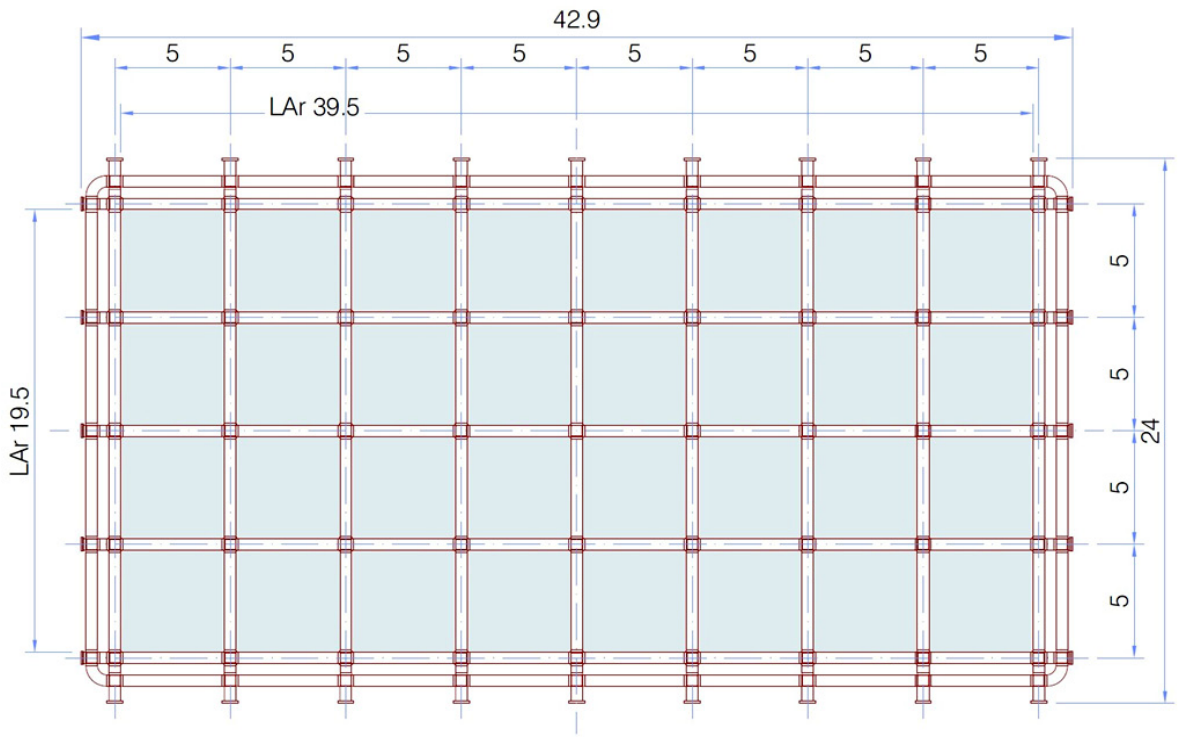

Figure 3

The distributed thermal stabilization is combined to distributed argon **purification in liquid phase** based on multiple purification units. With 32 purification units in liquid phase (cryopumps + oxygen/moisture getter cartridges), distributed around the outer vessel, each with a 200 cm^3/sec pumping rate, the full liquid argon volume is passed through getter cartridges in one month and will continue to be purified as needed.

An eventual passive insulation can be assembled around the outer vessel, if safety reasons require it.

3. Cryostat Construction and Assembly

The cryostat structure is based on repetition of few elements:

a) Square stainless steel beams (Figure 4):
   Number = 944 (560 for inner vessel, 384 for outer vessel)
   Cross section = 500 mm x 500 mm
   Wall thickness = 20 mm
   R_{in} = 20 mm
   Length = 4'300 mm
   Unit weight = 1285.6 Kg

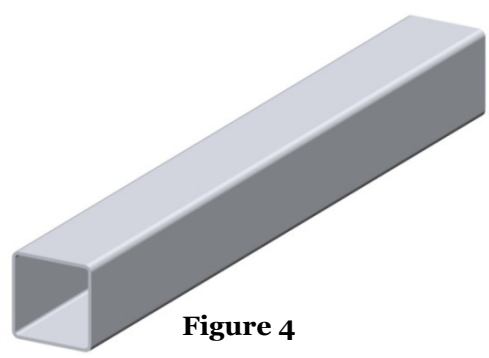

Figure 4

b) Tubular 6-way cross (Figure 5):
   Unit weight = 197.6 Kg
   Number = 455 (225 for inner vessel, 230 for outer vessel)
   Size = 520 mm x 520 mm x 520 mm
   Wall thickness = 20 mm

Figure 5

c) Tubular elbows (Figure 6):
   Number = 76 (for outer vessel only)
   R_{in} = 400 mm
   R_{out} = 900 mm
   Wall thickness = 20 mm
   Unit weight = 305.6 Kg

Figure 6

d) Double-skin ¼-cylinder walls (with frame and inner reinforcement, Figure 7):
   Number = 64 (for outer vessel only)
   Length = 4'700 mm
   Skin thicknesses = 5 mm
   Unit weight = 821.6 Kg

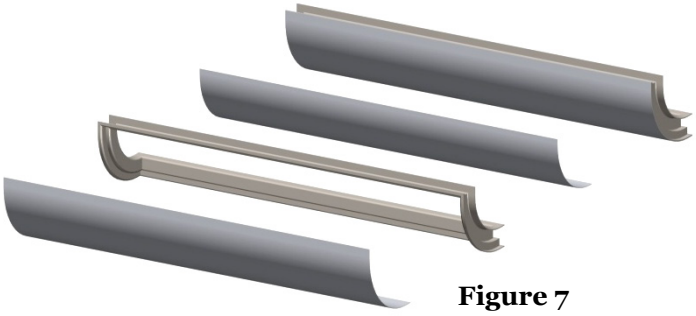

Figure 7

e) Double-skin square walls (with frame and inner cross-reinforcement, Figure 8):
   Number = 320 (160 for inner vessel, 160 for outer vessel)
   Size = 4'500 mm x 4'500 mm x 250 mm
   Skin thicknesses = 5 mm
   Unit weight = 2'829 Kg.

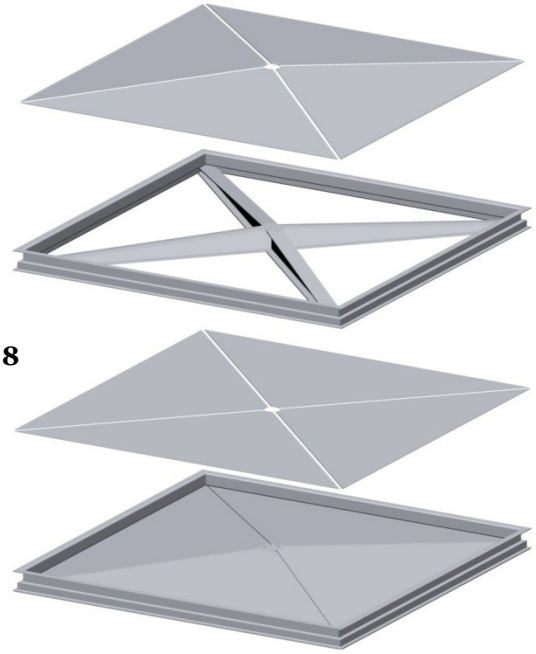

Figure 8

f) Double-skin ⅛ -sphere walls (with frame and inner reinforcement, Figure 9):
Number = 8 (for outer vessel only)
Unit weight = 196.8 Kg.

Figure 9

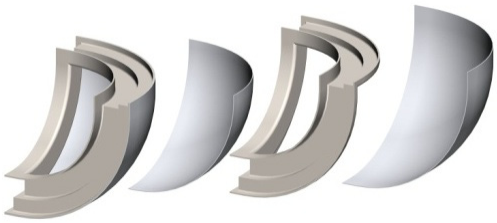

g) Feet (Figure 10):
Number = 45 (for outer vessel only)
Unit weight = 375.2 Kg

Figure 10

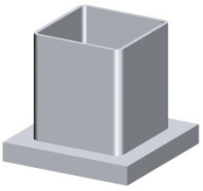

h) Side thermal bridges (Figures 12 and 13): Number = 230

Sizes and weights in the above list are based on a preliminary CAD design and are given here as an indicative/conservative hypothesis. They must be optimized by a dedicated engineering study and R&D tests. All details are foreseen to be built outside (mechanical construction and welding company) and brought underground.

The cryostat is assembled underground. Main operation is welding the different details by TIG (or laser[1]) welding machines.

Dedicated CNC welding stations are required. After welding square beam and crosses, the walls are welded from inside and outside. The most difficult part appears the assembling of the lower sides of outer and inner vessels, for which, after welding SS square beams and crosses, the double skin walls should be welded from top and bottom.

Solution for this operation is the use of a 250-300 ton truck crane, or equivalent (Figure 11), to position each one of these sides (224 ton for the outer lower side and 215 ton for the inner lower side) for an easy welding on both sides.

With the bottom face in its final position, it becomes the base from which it is possible mount the vertical lower thermal bridges and on them proceed with the inner lower face. From this point the assembling procedure becomes more linear and repetitive.

Leak detection must be planned after welding details as square beam structure and dual-skin windows. Vacuum tightness inside the wall and the beam structure of the inner and outer vessel and of the in-between space is a guaranty for the full cryostat vacuum tightness.

[1] Laser welding performances are described, as example, in a video of Montanstahl® (http://www.montanstahl.de/de/download/laserschweissen/support: Film über deformierende Prüfung eines Laserprofils.wmv).

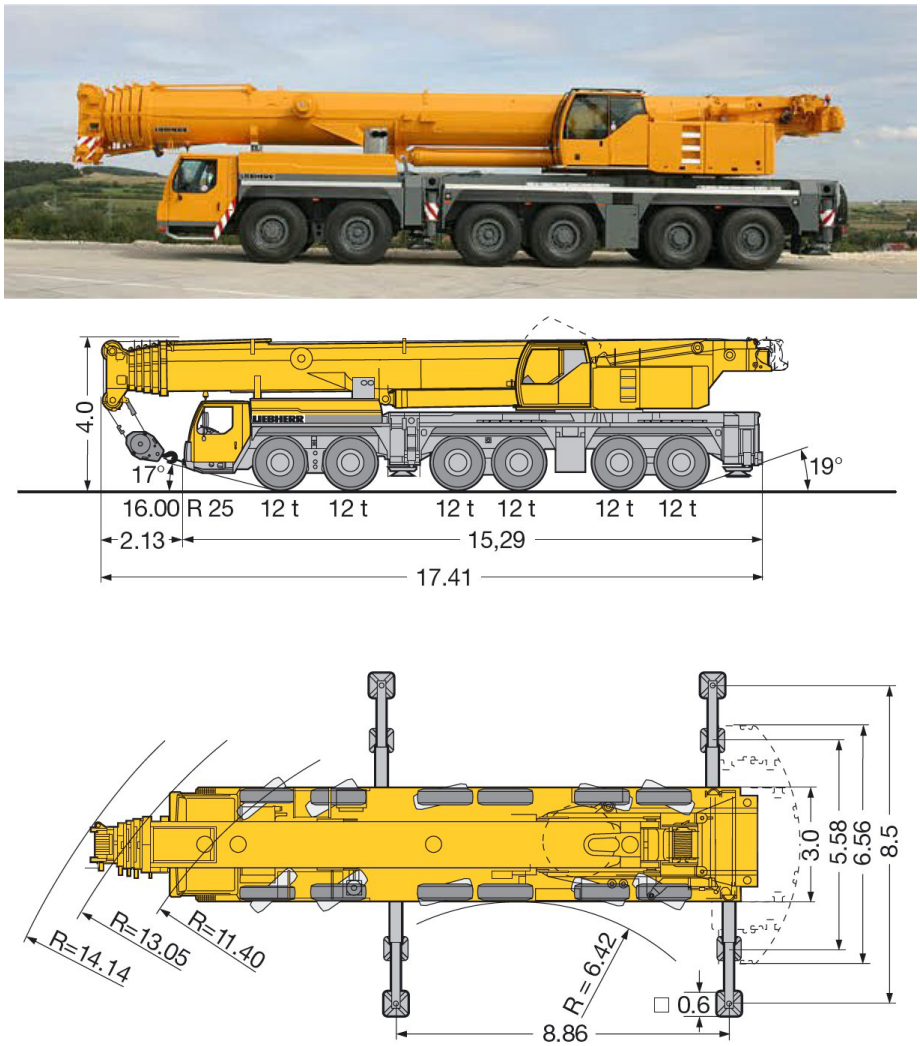

Figure 11 – LIEBHERR LTM-1250 250 ton truck crane

Thermal bridges are used to ensure the spacing between warm and cold structures. They are positioned on each warm beam cross.

For side and top faces they are made by insulating supports (Figure 12), with insulating beams made by a stack of thick fiberglass layers interleaved with thin stainless steel plates for mechanical load uniform distribution.

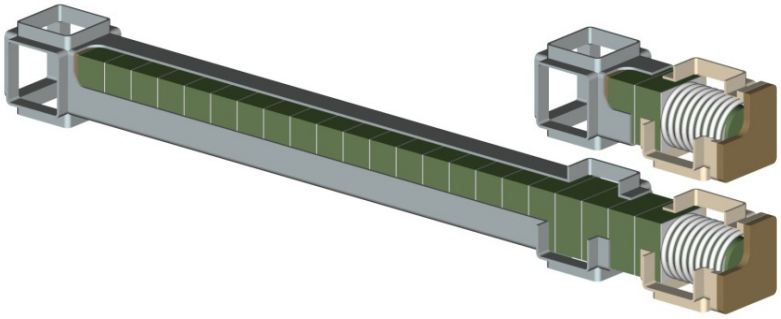

Figure 12 – Horizontal thermal bridges. Top: “short” at structure levels 1 and 5. Bottom: “long” at levels 2, 3 and 4.

They must be combined with elastic sections made by compression springs to accommodate the thermal shrinkage of the inner vessel with respect to the outer one. For the same purpose sliding pads are required, with a fixed reference link point in the central lower thermal bridge. On top and bottom faces thermal bridges are made by coaxial stainless steel tubes with a warm-to-cold end distance of 6 m (Figure 13).

The volume inside the beam structure and inside the double-skin walls is conveniently used as **heat exchanger**, by filling it with liquid nitrogen. A distributed LN_2 circuitry with separated volumes at different cryostat level can be implemented. As option for mechanical stability, pressurization of the outer vessel beams and walls at 0.5 bars can be considered.

The full outer surface of the inner vessel will be wrapped by 60-layer **super-insulation**. The super-insulation is kept in position by glass fiber fastenings and screw eyelets. For safety reasons, 4 (2) **expansion vessels** (ø = 2 m, L = 16 m) on the top of the cryostat are foreseen to provide a 1% (0.5%) expansion volume for the liquid argon in the detector. As mentioned above, the liquid argon thermal stabilization is provided by a LN_2 filled heat exchanger.

The residual heat transfer by conduction in thermal bridges is evaluated at 1.2 kW. With a total radiation heat absorbing surface of 4096.5 m^2 and a residual heat transfer of 0.6 watt/m^2, the heat input by radiation is about 2.5 kW. The total heat input results of the order of 3.7 kW.

This power is easily compensated by a **cryogenerato**r as the type SPC-4 produced by Stirling® (Figure 14) able to absorb a heat power of about 5 kW at 90K (Figure 15). Two of such cryogenerators are needed for periodic maintenance and to have a spare unit in case of trouble. Cooling water circuit, for 4000 l/h, and electric power for 43 kW are needed for such a cryogenerator.

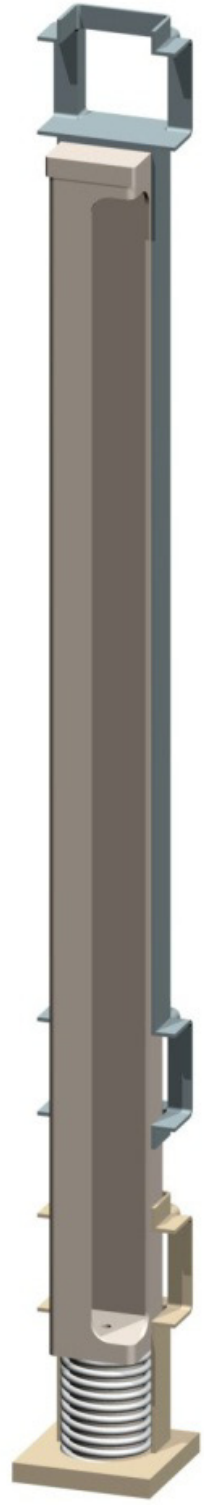

Figure 13 – Vertical thermal bridge.

Figure 14 – Stirling® SPC-4 cryogenerator

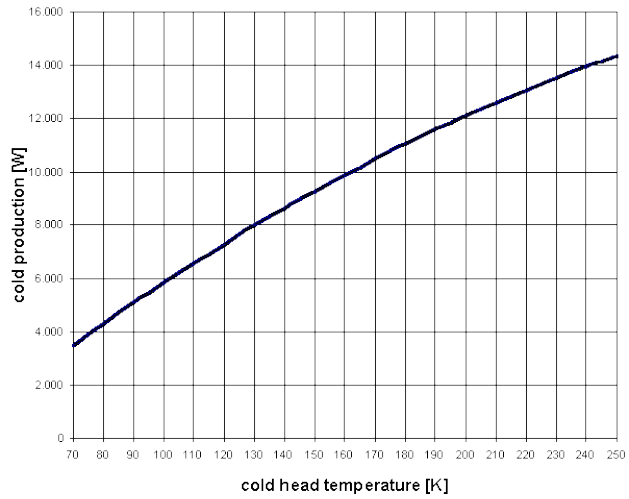

Figure 15

4. Detector configuration

The inner detector is configured as a set of 4 horizontal drift volumes, separated by cathode planes and each with a double side wire chamber at half height.

Schematic configuration of a wire chamber plane is shown in Figure 16. We propose a reading of each drift volume by two wire planes, the first with wires at 0° and the second with wires at 90°. This solution, based on an orthogonal / uncorrelated coordinate system, results as built by all equal length wires (maximum S/N ratio) and in a very practical and simple assembling: wires of each coordinate assembled and tensioned independently from the second coordinate.

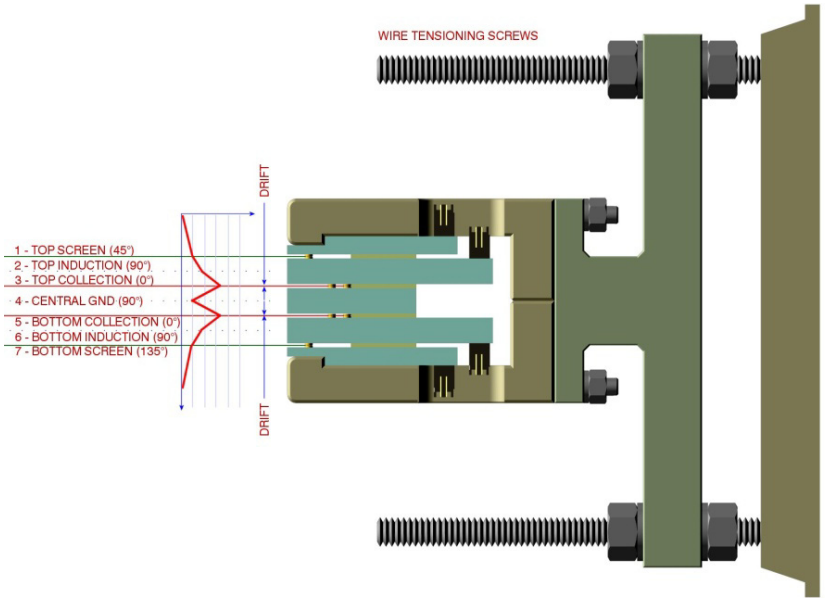

Figure 16 – Two-face wire chamber configuration.

Each drift volume over and under a wire chamber, is read by an “Induction” and a “Collection” wire plane. In order to read the volume between the two collection planes an intermediate wire plane can be inserted acting as low-voltage “cathode” plane. Optionally a “Screen” wire plane can be installed over the top induction plane and under the bottom induction plane. “Screen” planes and “Cathode” plane are not read passive elements, simply biased at the proper voltage. Chambers, seen from top, result as shown in Figure 17.

Wire tensioning supports are shown in Figure 18.

With a wire pitch of 3 mm and a wire diameter of 100 μm (working hypothesis), the single wire capacitance results 197.4 pF for a wire length of 9.5 m. This ensures very low electronic noise in each wire.

The total number of active wires in a plane results to be 25’416 and 406’656 for the whole detector (full wire length ~5’000 km!).

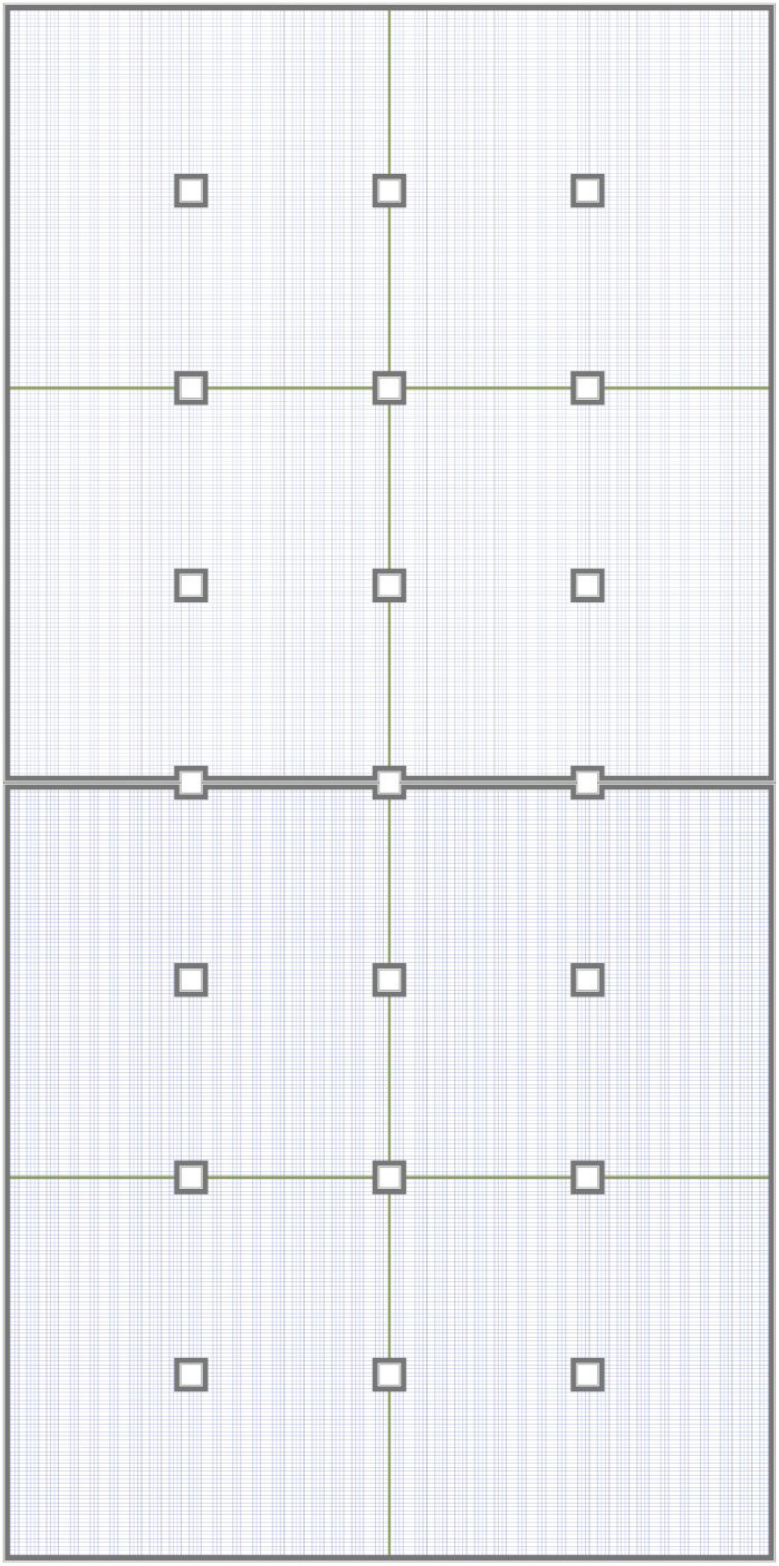

Figure 17 – Top view of a wire chamber plane.

As second option, a wire length of 19.4 m can be considered, with a capacitance increased to 401 pF/channel (still acceptable!) and half number of channels: 203'328.

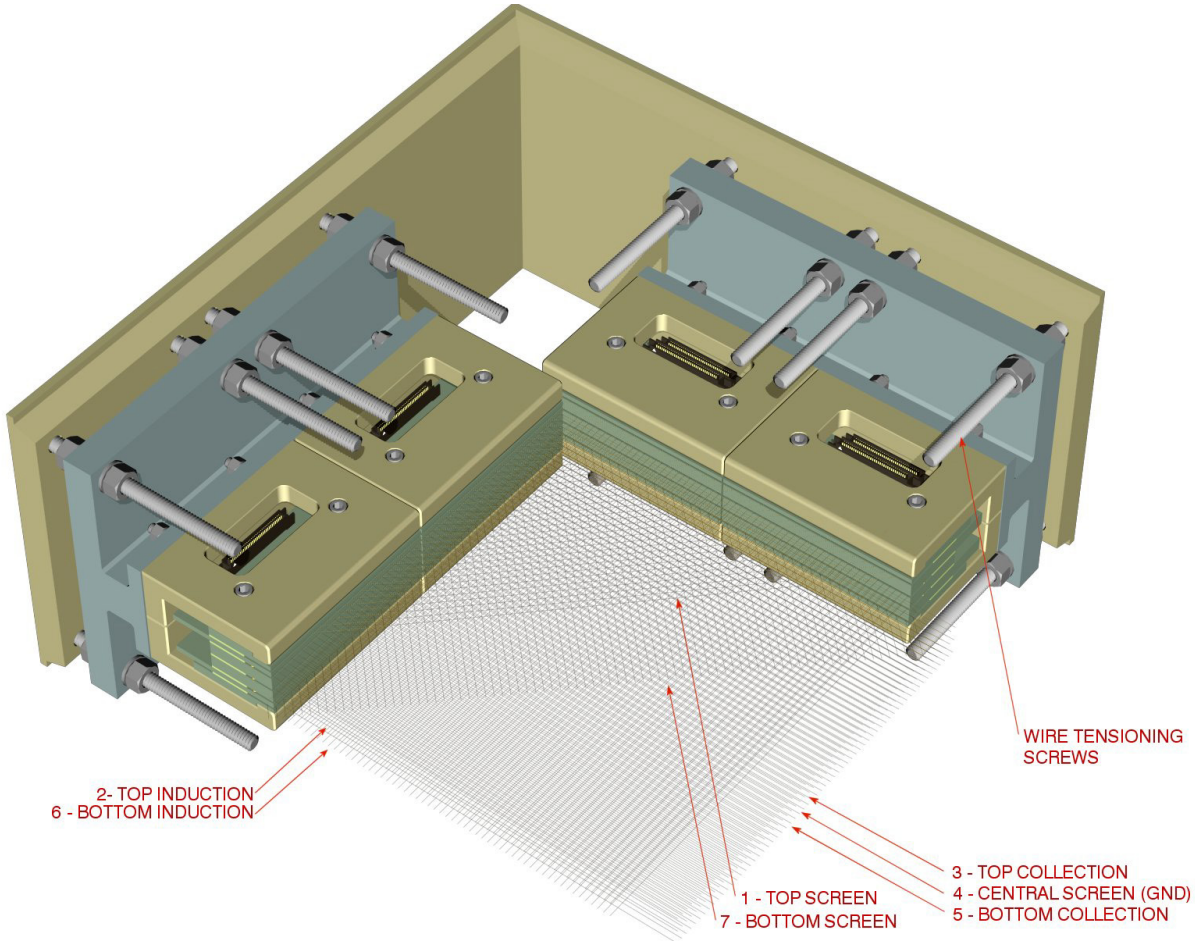

Figure 18 – Tensioning wire chamber supports.

The 4 wire chambers are located at heights of 2.13 m, 7.13 m, 12.13 m and 14.26 m (see Figure 20) from the bottom of the inner vessel. Figure 19 shows the left half of the inner detector. Cathode planes are located at ~0 m, 4.63 m, 9.63 m, 14.63 m and 19.26 m from the bottom of the inner vessel.

High voltage field shaping electrodes (FSE) surround the full drift volume (Figure 19) to guarantee an uniform drift field, by screening it from the inner beam structure (at ground voltage). Efficient screening and good field uniformity are obtained with FSE built of ϕ90 mm stainless steel tube at a vertical pitch of 124.3 mm. About 29.3 km of such tube are required (129.6 t for a ϕ 90×86 mm^2 tube).

FSE are supported by glass fiber supports linked to the inner vessel structure (total volume = 14.9 m^3, total weight = 28.3 t).

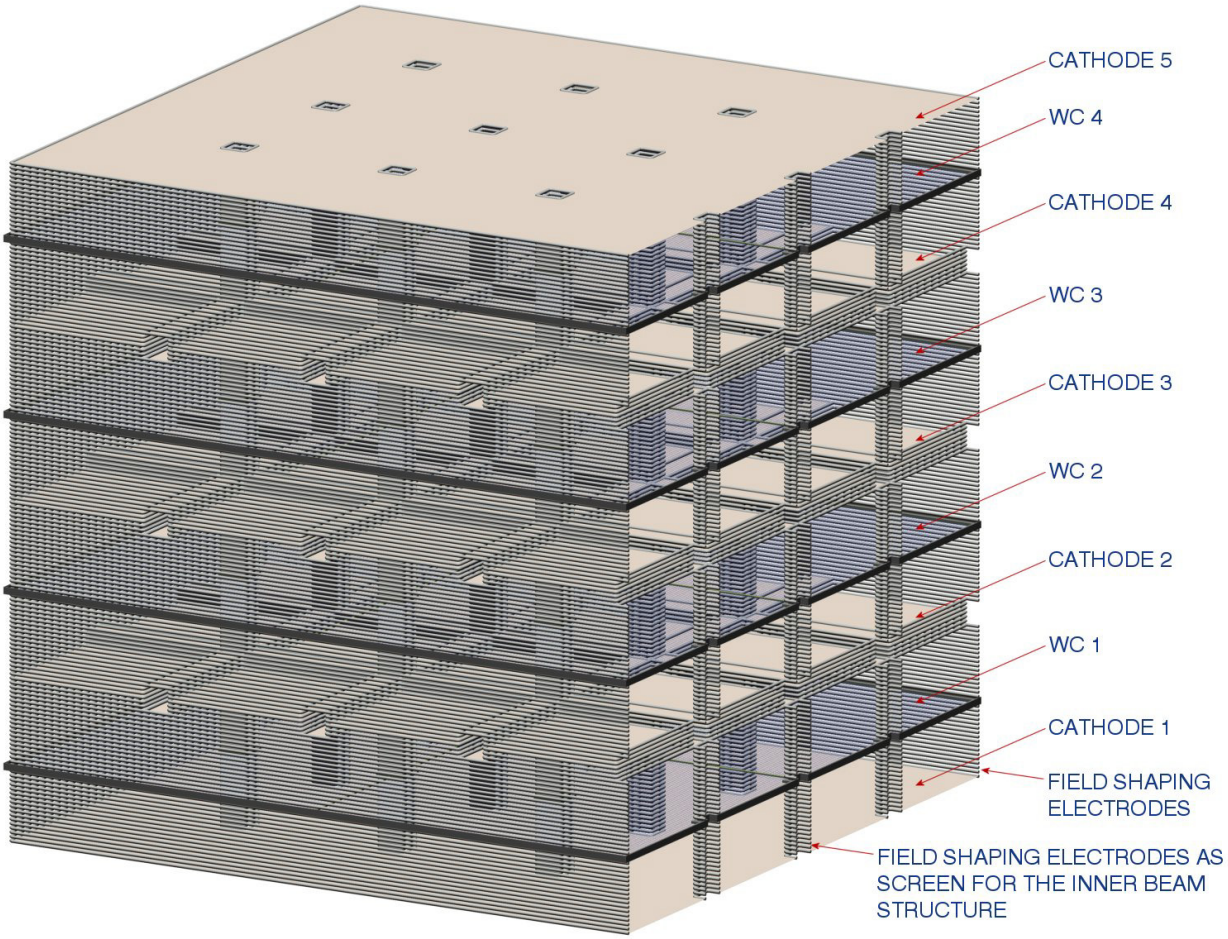

Figure 19 – Left half inner detector.

5. Detector construction and assembly

The detector, as described in Section 4, is made only by linear or small size elements: insulating FSE supports, FSEs, support plates for wire end PCBs with tensioning screws, rolls of multiple wires (32, 64 or 128) pre-mounted on PCB plates, cathode plane elements (thick wires or perforated plates). These elements are easy to transport and to introduce inside the inner vessel. During the detector assembling the cryostat is then used as clean room with manholes and fresh air ventilation.

Assembly starts from top, with temporary bridges under the working level, and ends over the lower cathode plane.

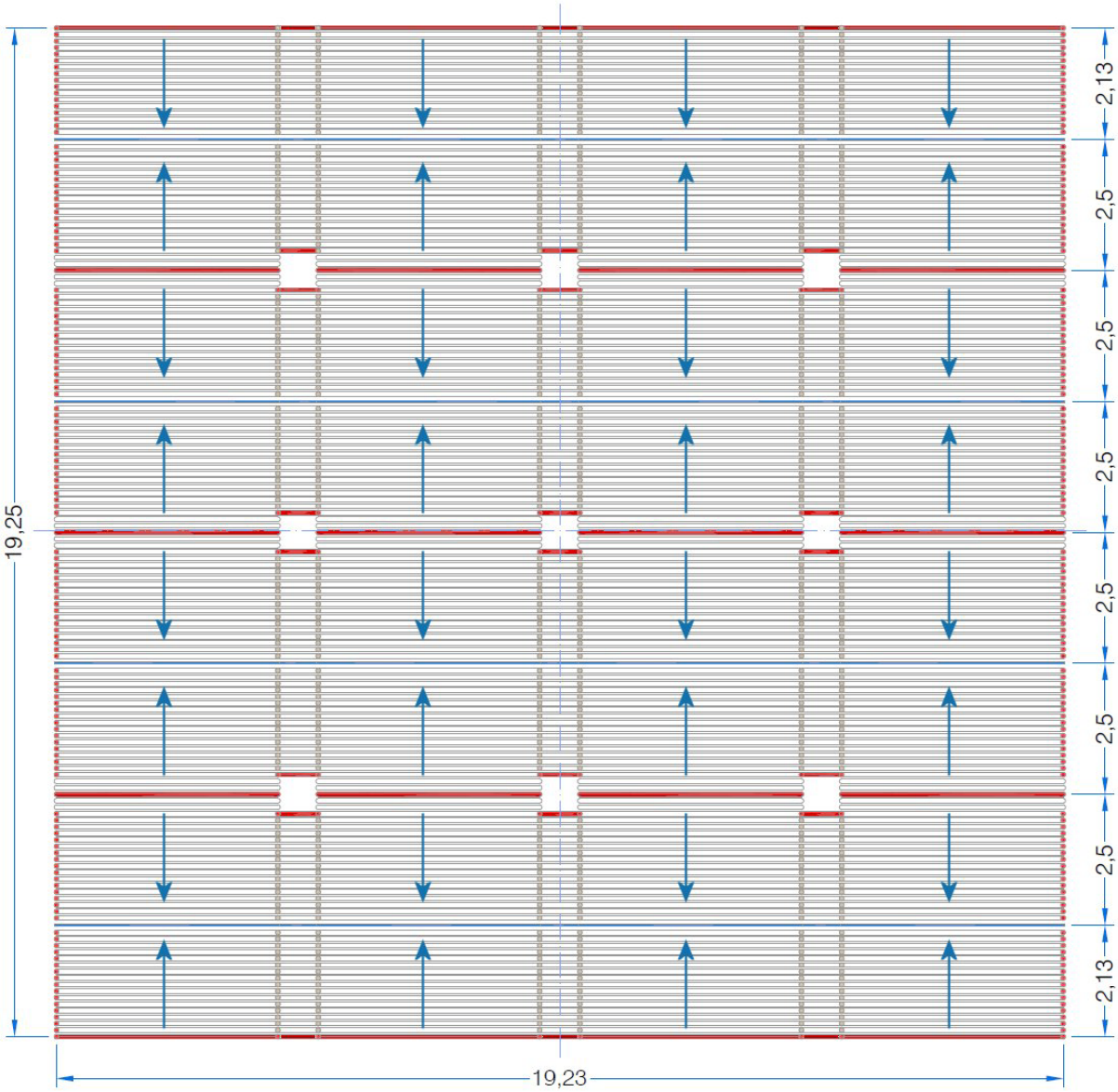

Figure 20 – Inner detector vertical cross section. Arrows indicate electron drift directions.

6. Detector in the underground hall

The cryostat overall dimensions are about L = 43 m × W = 23 m × H = 23 m. Minimum width of the cavern is W_c = 24 m and minimum length is L_c ≈ 48 m to have a space in front of the cryostat to lower, by a bridge crane or a truck crane, welding machines, tools, leak detectors, vacuum pumps, cryostat and detector details in front of a temporary entrance in the cryostat walls (Figure 21 and 22).

For safety reasons, entrance tunnel and normal operation counting rooms are located at the top level of the cavern.

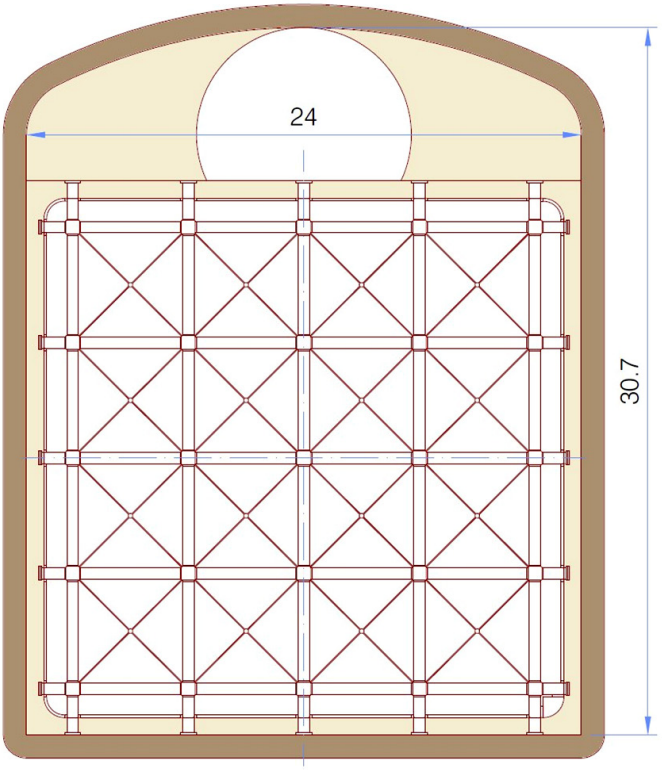

Figure 21 – Front view of the detector inside the cavern.

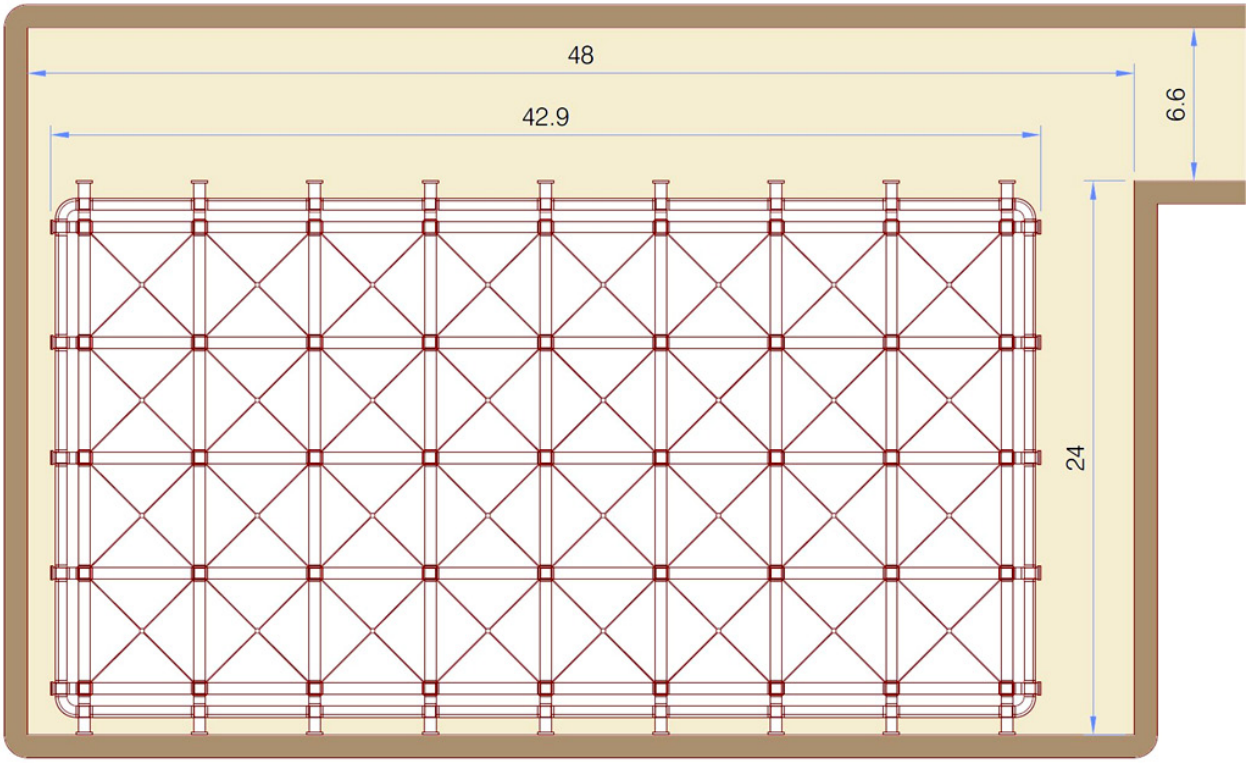

Figure 22 – Side view of the detector inside the cavern.

An unexpected argon leak will fill the bottom of the cavern giving alarms by O_2 concentration sensors, allowing people to evacuate in full safety. A gas tight door must be installed for this purpose across the top entrance tunnel.

7. Cost estimate

Cost for liquid argon strongly depends on its transport expenses.

The total volume of liquid argon inside the cryostat results 15□159.5 m^3.

The gas argon inside the cryostat is 136.1 m^3 (0.88% of the liquid volume).

The instrumented (with electric field) liquid argon volume is 13□853.3 m3 (91.4% of the total liquid argon).

The linearly instrumented liquid argon volume is 13 □094.7 m^3 (86.4% of the total liquid argon).

The fiducial volume (as fiducial target volume: events initiated inside it are fully contained in the linearly instrumented volume) depends on the events type, energy, direction and on dead spaces inside the active volume. The proposed configuration has continuous linearly instrumented liquid volume across the cryostat inner beam structure, with minimized broken regions and maximized fiducial volume. As example, for events in a horizontal plane, with a direction at 45° respect to the detector long size, "fully" contained in a cone with base diameter of 2 m and height of 3 m, the fiducial volume results 5□885 m^3 (8.24 kton, 39% of the total liquid argon).

Numbers and weights for cryostat and detector main components are listed in Table 1, with a rough estimate of the costs for materials, machining, welding and assembling (on sureface and underground). Cost for electronics, cables and connectors, crates, racks, LV/HV power supplies, signal and HV feedthoughs and electronic instrumentation are not included.

Table 1

Description	Number	Unit weight, t	Total weight, t	Estimated cost, k$
Cryostat				
Inner vessel material				
SS square pipe beams, 500 mm × 500 mm, t = 20 mm, L = 4300 mm	560	1.286	719.9	
SS square pipe 6-way crosses, 520 mm × 520 mm× 520 mm, t = 20 mm	225	0.198	44.5	
SS 2-skin square walls, 4'500 mm × 4'500 mm× 250 mm, (frame and 5 mm thick plates)	160	2.829	452.6	
Outer vessel material				
SS square pipe beams, 500 mm × 500 mm, t = 20 mm, L = 4'300 mm	384	1.286	493.7	
SS square pipe 6-way crosses, 520 mm × 520 mm× 520 mm, t = 20 mm	230	0.198	45.5	
SS tubular elbows, R_{in} = 400 mm, R_{out} = 900 mm, t = 20 mm	76	0.306	23.2	
SS 2-skin square walls, 4'500 mm × 4'500 mm× 250 mm, (frame and 5 mm thick plates)	160	2.829	452.6	
SS 2-skin ¼ cylinder walls, (frame and 5 mm plates), L = 4700 mm	64	0.822	52.6	
SS 2-skin ⅛ sphere walls, (frame and 5 mm plates),	8	0.197	1.6	
SS feet	45	0.376	16.9	
SS thermal bridges	90			
Total SS			2'303.1	20'000
Stratified Glass Fabric thermal bridges	140			140
Multilayer Superinsulation for the inner vessel (40 layers, 4'000 m^2)				700
Inner and outer vessel working				
Machining				5'000
Linear welding for beams and walls				5'000
Flanges for feedthroughs				
Liquid phase purification units (cryopump, getter cartridge)	36			2'000
LAr circuitry and valves				
LN_2 circuitry and valves				
LAr and LN2 buffers				
Cryogenerators (of the type STIRLING® SPC-4)	2			550
Vacuum pump groups (of the type VARIAN® Turbo-V 3K-T with TriScroll 600)	8			280
Detector				
Readout wires (ϕ = 100 µm, L = 5'000 km, single wire length = 19.4 m)				
PCBs (128 wires/PCB pair)	3'180			
Ferrules, number = 5.15 M				
LV cathode wires (ϕ = 100 µm, L = 2'500 km, single wire length = 19.4 m)				
PCBs (128 wires/PCB pair)	1'590			
Ferrules, number = 2.6 M				
Screen wires (ϕ = 100 µm, L = 5'000 km, single wire length = 19.4 m)				
PCBs (128 wires/PCB pair)	3'180			
Ferrules, number 5.15 M				
FSE tubes (ϕ = 90 x 86 mm, total length = 29.3 km)				1'600
FSE insulating supports, 28.3 t				850
HV resistors for the voltage degrader	1000			25
Total				**36'145**